J Mater Sci (2007) 42:5964–5972
DOI 10.1007/s10853-006-1110-8

Epoxy composites with 200 nm thick alumina platelets as reinforcements

Dharmendra Kumar Shukla · Venkitanarayanan Parameswaran

Received: 27 June 2006 / Accepted: 5 October 2006 / Published online: 6 April 2007

Abstract Composites were prepared by dispersing Alumina platelets of polygonal shape having a thickness of 200 nm and size of 5–10 μm in epoxy (LY 556) matrix using sonication. Good dispersion of the platelets was observed through scanning electron microscopy (SEM). The quasi-static plane-strain fracture toughness and tensile properties of the composites were determined for platelet volume fraction varying from 0% to 10%. The results indicated that addition of the platelets give considerable improvement in fracture toughness and good improvement in the elastic modulus of epoxy. For 10% volume fraction of the platelets, the fracture toughness improved by 110% where as the improvement in elastic modulus was 78%. However there was an associated reduction of 53% in tensile strength and 73% in failure strain. SEM of fractured surface was carried out to understand the various mechanisms responsible for the improvement in fracture toughness. By appropriately accounting for the orientation and stacking effects of the platelets, the applicability of predictive models, such as the Halpin-Tsai and Mori-Tanaka, for estimating the composite modulus is demonstrated.

Introduction

Polymers are used extensively in various applications such as food packaging, construction and building material, light weight structural components, automotive parts, biomedical applications and as matrix material in fiber composites. However, usage of un-reinforced polymer is restricted primarily to non-safety-critical components because of their inferior mechanical properties in comparison to metals. Fiber reinforced composites with thermosetting polymers such as epoxy and polyester as matrix material, have become quite a match for the metals in recent years. The highly cross linked and coordinate bonded structure of these polymers provide good mechanical and thermal properties, but at the same time makes them extremely brittle and thus poor inhibitors of crack initiation and propagation.

Reinforcing polymers with rigid particles have been conventionally attempted to enhance their stiffness and toughness. With the availability of particles in the nanometer size range, recent studies have focused on using nanoparticles to improve the properties of both thermoplastics and thermosetting resins. Kojima et al. have shown an improvement of 100% in elastic modulus of nylon 6 by dispersing 4.2% of nano-clay as early as 1993 [1, 2]. Subsequently many researchers have achieved improvements in mechanical and thermal properties by dispersing nano-clay in various polymer matrices such as polyimide, polyurethane, epoxy, nylon 6 and agarose [3–7].

In a recent study, Daniel et al [5] reported moderate increase in the elastic modulus and tensile strength of epoxy-clay nanocomposites at very low volume fraction of clay. However, at higher volume fraction (10%) the elastic modulus increased by 90% whereas the tensile strength decreased by 44%. The fracture behavior of epoxy nanocomposites reinforced with α-Zirconium phosphate was investigated by Sue et al. [6]. They reported improvements in strength, modulus and fracture toughness. Very recently, Xiaodong et al. [7] have reported a sixfold increase in elastic modulus and 50% increase in the tensile strength of

D. K. Shukla · V. Parameswaran (✉)
Department of Mechanical Engineering, Indian Institute of Technology Kanpur, Kanpur 208016, India
e-mail: venkit@iitk.ac.in

agarose films reinforced with 60% (wt) of nano clay. Chisholm et al. [8] also achieved a 45% increase in the elastic modulus of epoxy by adding silicon carbide nanoparticles.

The effect of dispersing metal and metal oxide nanoparticles on the fracture properties of thermosetting polymers has also been studied recently [9–12]. Park et al. [9] studied the effectiveness of the ultrasonic method to disperse iron oxide nanoparticles in epoxy vinyl ester matrix and identified the appropriate processing parameters that would give uniform particle dispersion without agglomeration. Singh et al. [10] investigated the effect of particle size (ranging from 20 μm to 100 nm) on the elastic and fracture behavior of polyester particulate composites. Zhang and Singh [11] reported that, by improving the interfacial bond between nanoparticles and the resin the fracture toughness can be improved by 100%. Evora and Shukla [12] achieved an increase of 57% in fracture toughness of unsaturated polyester by the dispersion of 40 nm size TiO_2. However, there was no appreciable improvement in the elastic modulus in the investigations cited above.

In most of the studies discussed so far, the size of the particles used was either completely in the nano-range i.e. the thickness and in plane dimensions of the clay platelets or diameter of spherical particle were in nanometer length scale. In the present study, alumina platelets of thickness 200 nm and in plane dimensions in the range of 5–10 μm have been selected as the reinforcement. This system therefore has a mixed length scale with an aspect ratio in the range of 25–50. The effects of adding platelets on both the fracture toughness and tensile properties of epoxy are then determined. Analysis of fractured surface of nanocomposites using scanning electron microscopy (SEM) has been carried out to identify the different mechanisms responsible for improvements in the fracture toughness. The applicability of some existing models for predicting the elastic modulus of the composite is also demonstrated.

Experimental details

Composite preparation

Alumina platelets used in this study were procured from Advanced Nanotechnology Ltd., Australia. These platelets having a density (ρ) of 3.97 gm/cc were of polygonal shape having in plane dimension in the range of 5–10 μm and a thickness of 200 nm. An SEM photograph of the platelets is shown in Fig. 1. It can be seen that these are irregular polygons.

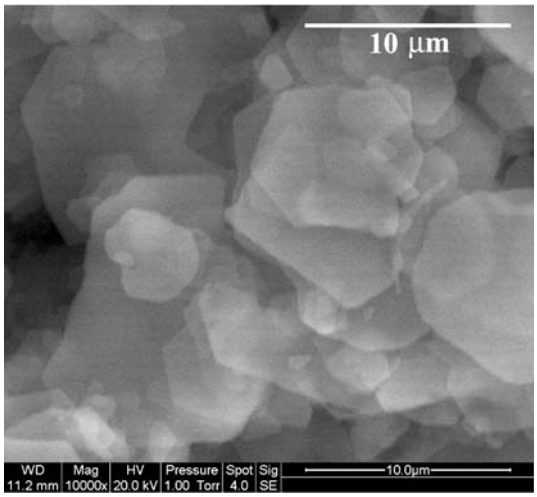

Fig. 1 SEM photograph of alumina platelets

The platelets have an aspect ratio in the range of 25–50. The surface area per unit weight (λ) of these platelets can be written as

$$\lambda = \frac{2}{\rho t} + \frac{P}{\rho A}$$

where t is the thickness, P is the perimeter of the cross section and A is the face area. For the aspect ratios considered here, the second term ($P/\rho A$) can be neglected and therefore we have $\lambda = 2.52\ m^2/gm$ for the platelet. A spherical alumina particle having diameter of 200 nm, will have a $\lambda = 7.56\ m^2/gm$ which is three times that of the platelets. The epoxy and hardener used were *Araldite LY556*® and *LY951*®. These were supplied by Vantico Performance Polymers Pvt. Ltd., India. LY556 having a density of 1.17 gm/cc is an unmodified liquid epoxy resin based on Bisphenol A and the hardener LY951 having a density of 0.98 gm/cc is an aliphatic primary amine.

The required amount of dry alumina platelets corresponding to the desired volume fraction was first mixed with epoxy resin (LY556) for a duration of 10 min. Then the mixture was sonicated for 30 min using an acoustic probe of 13 mm diameter driven by a Sonics Vibra Cell® ultrasonic processor. Sonication was carried out at 75% amplitude. To avoid heat build up in the mixture, sonication was done in pulsing mode of 5 s on and 9 s off. The mixing beaker was kept in a mixture of ice and water and the temperature was not allowed to exceed beyond 35 °C during the sonication process.

After sonication the mixture was kept in vacuum for 25 min to remove air bubbles entrapped during mechanical mixing and sonication process. Then hardener LY951, in the ratio of 1:10 by weight of resin, was added and mixed without entrapping air bubbles. The final mixture was

poured in vertical acrylic moulds and was cured at 26 °C for 24 h. After this the composite was taken out of the mould and post cured at a temperature of 100 °C for 4 h and was allowed to cool to room temperature in the oven itself. For the hardener ratio used in this study, the resin gelled in 40 min and no settling of particles was observed during the time elapsed between sonication and gelling. By this procedure, composites having platelet volume fraction of 0.5, 1.0, 5.0 and 10% (1.7%, 3.4%, 15.4% and 7.7% weight fraction) were prepared.

The density of the composite was measured by taking samples from different locations along the height of the mold. There was hardly any variation in density indicating that the platelets did not settle due to gravity. Further to this SEM images of the composites were taken to investigate the dispersion of the platelets in the matrix. These SEM micrographs for the different platelet volume fractions are shown in Fig. 2. It is clear from Fig. 2 that the platelets are dispersed homogeneously in the epoxy matrix and have random orientation. At higher volume fraction (above 5%) platelets are stacked together at many locations as can be seen in magnified SEM images in Fig. 2e, f. It has been noticed that at most of the locations of stacking, on an average two platelets stack together in 5% whereas three or more platelets are stacked together in case of 10% platelet volume fraction.

Mechanical characterization

Characterization of tensile properties

Tensile properties of the composites were obtained following ASTM standard D 638-03 [13]. Test specimens of type I were directly molded to the specified shape. Gage length, width of narrow section and thickness of the specimens were 50, 13 and 6.5 mm respectively. Overall length and width were 165 and 19 mm. Strain of the gage section was measured using a clip gage. For each volume fraction, five tests were conducted using an INSTRON® machine at a crosshead speed of 5 mm/min. The elastic modulus, tensile strength and failure strain were then obtained from the test data.

Fracture characterization

The plane-strain fracture toughness of nanocomposite was measured in terms of critical stress intensity factor (K_{IC}) following ASTM standard D 5045-99 [14]. The length, width and thickness of the three-point bend specimens were 57.2, 13, and 6.5 mm, respectively. Specimens of these dimensions were machined from the cast sheets of composite using a high-speed diamond saw equipped with water-cooling. After that an initial notch of width 0.3 mm was created in the specimens by machining using the diamond saw. Thereafter, a natural crack was created by tapping a sharp razor blade into the initial machined notch. The overall length (machined + natural) of the crack was kept between 0.45 and 0.55 times of the specimen width. For each volume fraction, ten samples were tested at a crosshead speed of 10 mm/min. The fractured specimens were inspected in an optical microscope to measure the actual crack length. Results from the specimens in which the natural crack did not meet the ASTM specifications were discarded. The average fracture toughness and 95% confidence level were then calculated for each volume fraction.

Results and discussion

The addition of the platelets increased the density of the composite. The density of 10% platelet composite was 22% higher than that of neat epoxy. The stress–strain response of composites prepared is shown in Fig. 3. The response of all composites is linear in the beginning from which the elastic modulus was calculated through regression. As the platelet volume fraction increases, the slope of this initial portion increases indicating an increase in the elastic modulus. Pure epoxy has a considerable non-linear portion from about 1% strain to the failure strain of 3%. The 0.5% and 1.0% platelet composites, also exhibits non-linearity in the stress–strain response beyond 1% strain where as the non-linear portion is considerably less for 5% and 10% case. The final failure was brittle in nature for all the composites.

Tensile properties of the composite for different volume fraction of platelets are shown in Figs. 4–6. Figure 4 shows the elastic modulus as a function of platelet volume fraction. Volume fractions of 0.5%, 1%, 5% and 10% alumina platelets showed 6%, 19%, 58% and 78% increase in elastic modulus in comparison with that of neat epoxy. The constraint imposed by the rigid platelets on the local matrix deformation field gives rise to the increase in the modulus. The platelets are randomly oriented and hence the material behavior at the bulk scale can be assumed to be isotropic. However, there could be anisotropy at length scales comparable to the size of the platelets and this aspect is discussed later in the section on modeling.

Both tensile strength and failure strain decreases with increasing platelet content as indicated in Figs. 5, 6. Only the results from tests in which the failure occurred in the gage section are reported. For 10% platelet content the tensile strength reduced by 53% and there was a reduction of 73% in the failure strain. This behavior is typical of thermosets reinforced with rigid micron sized particles. The tensile strength depends more on the load transfer

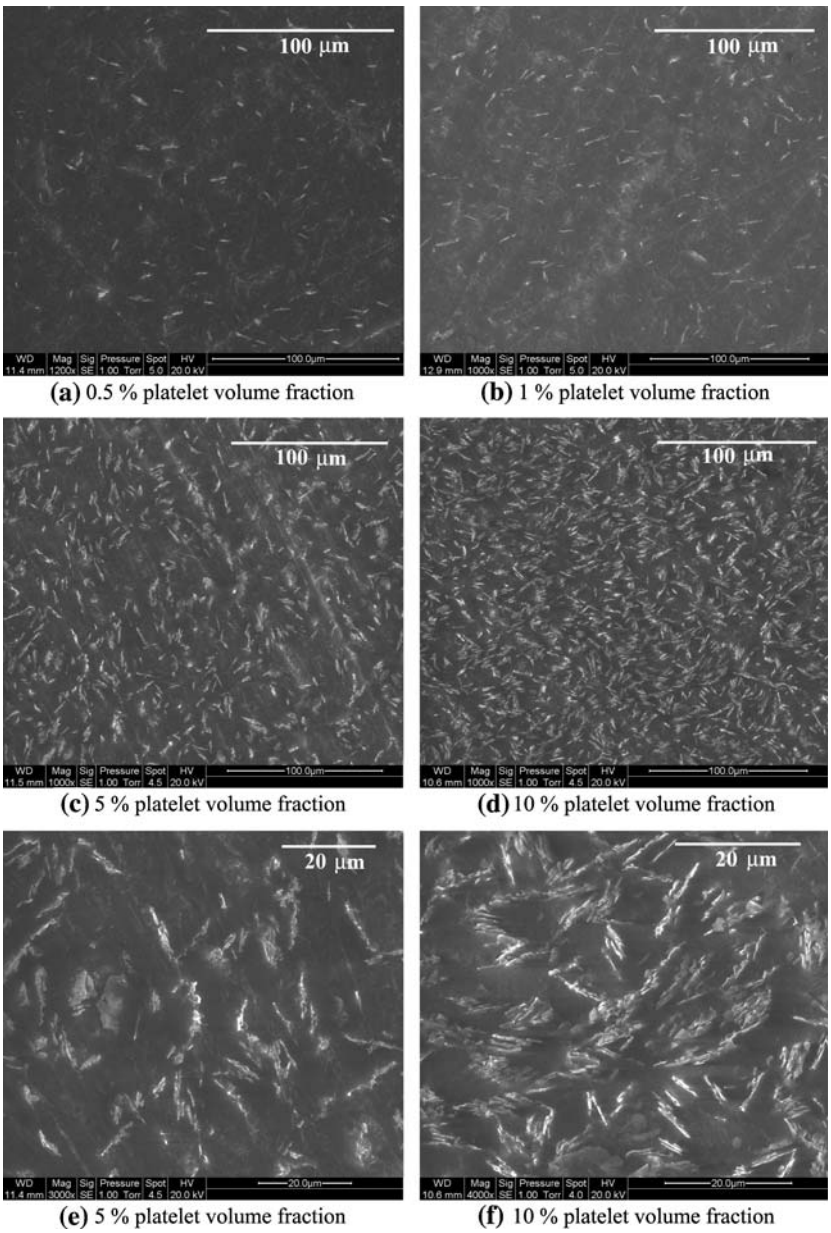

Fig. 2 SEM micrographs showing the distribution of alumina platelets in epoxy

(a) 0.5 % platelet volume fraction **(b)** 1 % platelet volume fraction

(c) 5 % platelet volume fraction **(d)** 10 % platelet volume fraction

(e) 5 % platelet volume fraction **(f)** 10 % platelet volume fraction

between the matrix and the platelets. In the present study the platelets were used as such without any surface modification and hence the interface between the matrix and the platelets is inherently weak. Therefore there will not be significant load sharing by the platelets and well-dispersed platelets are tantamount to penny shaped flaws of 200 nm nanometer thickness.

Another factor responsible for the reduction in the strength is the platelet stacking. In the 0.5% and 1% platelet composites, the platelets are well dispersed and there is little decrease in the tensile strength (9% and 11% respectively). At 5% and 10% volume fraction of platelets, stacking of platelets occurs (see Fig. 2e, f). These weakly bonded stacked platelets have an effective thickness in micrometer range and act as sites of stress concentration reducing the tensile strength significantly.

Figure 7 shows the variation of fracture toughness of the composites as a function of the volume fraction of platelets. It can be observed from Fig. 7 that addition of the platelets improves the fracture toughness of the resin. Volume fractions of 0.5%, 1%, 5% and 10% alumina platelets showed 36%, 56%, 98% and 110% increase in fracture toughness in comparison with that of neat epoxy. It is worth observing that this increase in the fracture toughness is substantial and is achieved without any surface treatment to increase platelet–matrix adhesion. In the case of thermosets reinforced with metallic oxide nanoparticles, the maximum improvement in fracture toughness

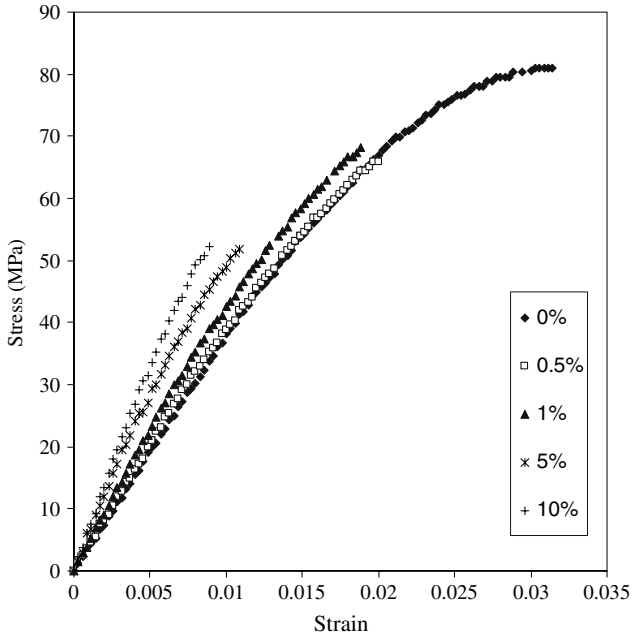

Fig. 3 Stress–strain curves as a function of platelet volume fraction

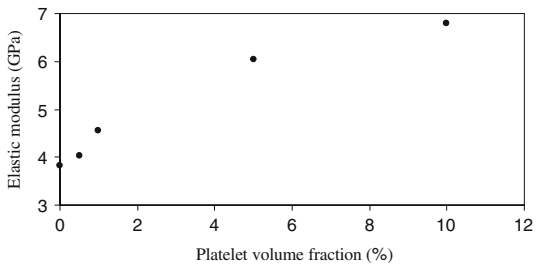

Fig. 4 Elastic modulus as a function of volume fraction of alumina platelets

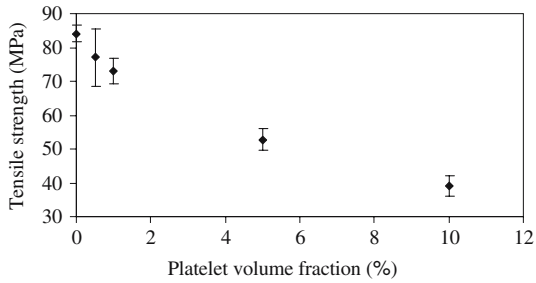

Fig. 5 Failure strength as a function of volume fraction of alumina platelets

has been observed at 1% volume fraction and there after the fracture toughness does not increase with increasing particle volume fraction [11, 12].

SEM of the fractured surfaces was carried out in order to understand the toughening mechanisms. Figure 8 shows the SEM micrographs of fractured surface for different

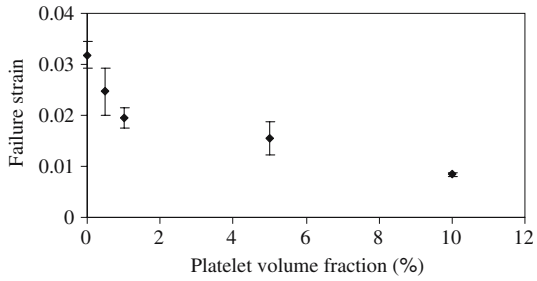

Fig. 6 Failure strain as a function of volume fraction of alumina platelets

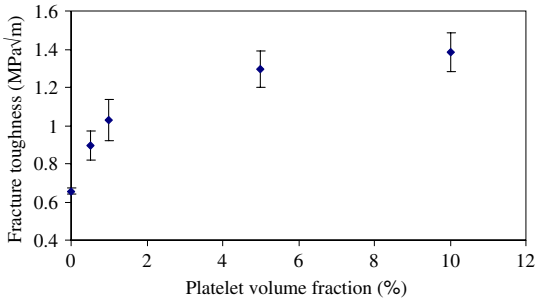

Fig. 7 Fracture toughness as a function of volume fraction of alumina platelets

volume fractions of alumina platelets taken slightly down stream (~0.5 mm) of the sharp crack tip. The overall crack propagation direction in Fig. 8 is from top to bottom. Some detailed fracture surface features are shown at higher magnification in Fig. 9. The fracture surface for epoxy (Fig. 8a) looks smooth and featureless. This indicates minimum energy for the fracture process and hence lower fracture toughness.

The fracture surface at lower platelet content (0.5% and 1%) shows primarily three distinct features; (1) tail lines (river marks) emanating from the platelet sites and extending down stream of crack propagation, (2) sites of empty platelets indicating clean pull out of the platelets from the matrix and (3) matrix spalling where the platelets have been pried out of the matrix (see Fig. 9a). The tail lines are formed when the crack front pins at the platelet and then subsequently circumvents the platelet and rejoins. When the plane of the platelet is oriented normal to both the crack surface and the crack front, only one tail line is seen, whereas when the plane of the platelet is normal to the crack surface but parallel to the crack front, a pair of tail lines can be seen. In composites with spherical reinforcements, typically only one tail line will be seen per particle at low volume fraction [10]. Even though, fracture is an instantaneous process at a macroscopic scale, the processes occurring in the fracture processes zone at the tip of the crack are not instantaneous, but progressive until the entire crack front propagates unstably. The presence of the

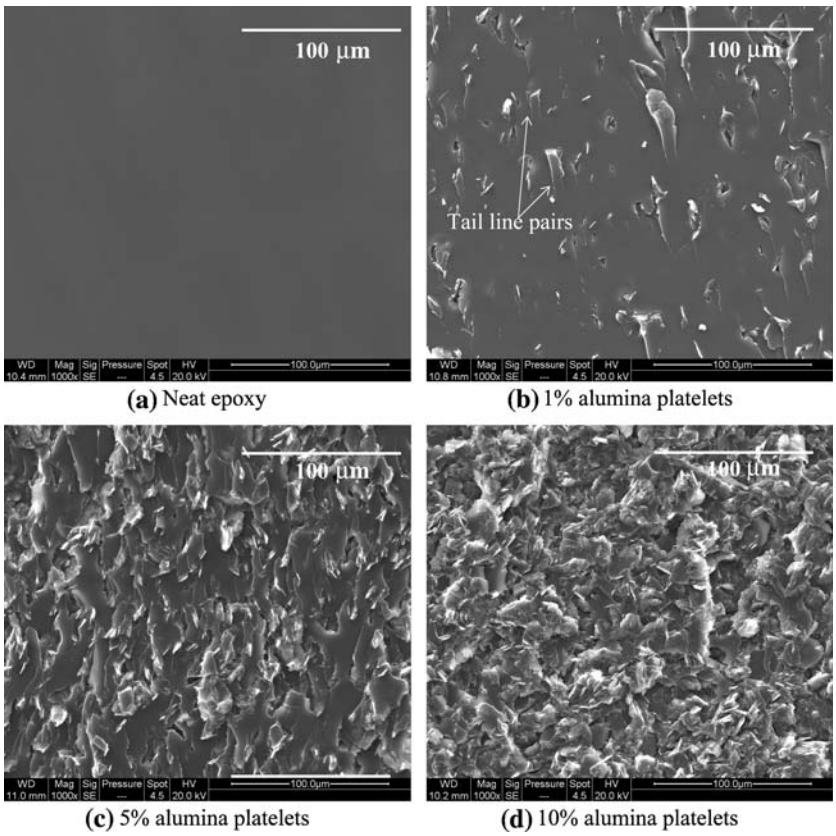

Fig. 8 SEM images of fractured surface

(a) Neat epoxy **(b)** 1% alumina platelets

(c) 5% alumina platelets **(d)** 10% alumina platelets

rigid particles can delay this unstable crack propagation by pinning and crack bridging. Pinning will allow the local crack front to extend stably consuming additional energy and alleviating the local stresses allowing the material to bear larger load.

The platelets will exert closing tractions on the crack faces leading to toughening by crack bridging. For the crack faces to finally open up during crack extension, either the crack will have to deflect along the matrix–platelet interface and switch to another plane avoiding the platelet altogether or debond from the platelet resulting in platelet pull out. The closing tractions exerted in the case of spherical particles will be of pure mode I type. However, in the case of platelets, the closing tractions will also have other mode components depending on the orientation of the platelet plane with respect to the crack surface and the crack front. Platelets with their plane parallel to the crack surface will be the least effective despite providing pure mode I type closing tractions, as the crack front can climb to the weak interface and extend through.

When the plane of the platelet is oriented at an angle to both the crack surface and the crack front, the closing tractions will have components corresponding to all three modes (mode-I, mode-II and mode-III). Other orientations could give either pure mode-I or combination of mode-I with either mode-II or mode-III. Thus the bridging effect is not as straight forward as that for spherical particles. For platelets with their plane oriented normal to the crack surface and either parallel or normal to the crack front, the closing traction will be purely mode-I type. When the crack faces open, these platelets will pull out cleanly without further matrix damage once the matrix has debonded completely from the platelet. Such pullouts will leave a crevice like feature on the crack surface as indicated in Fig. 9b. Platelets inclined to the crack surfaces cannot pull out freely even after they are debonded as they are wedged into the crack faces. The inclined platelets will be subjected to shearing and bending as the crack tries to open up [15, 16]. So these platelets will have to either break or be pried out of the crack faces. This will cause further matrix damage in the form of matrix spalling as shown in Fig. 9a. The platelets have much smaller embedded length in the matrix and therefore the frictional resistance during pullout is not as significant as in the case of random short fiber composites. Given the fact that the platelet matrix interface is not strong (as the platelets are not treated), the inclined platelets are more effective in bridging the crack which will not be the case with spherical reinforcements. So at low platelet volume fraction, crack trapping and crack bridging is believed to be the dominant toughening mechanism.

At higher volume fraction of alumina platelet (5% and 10%) the roughness of the fractured surface is significantly high. There are several steps and deep craters indicating

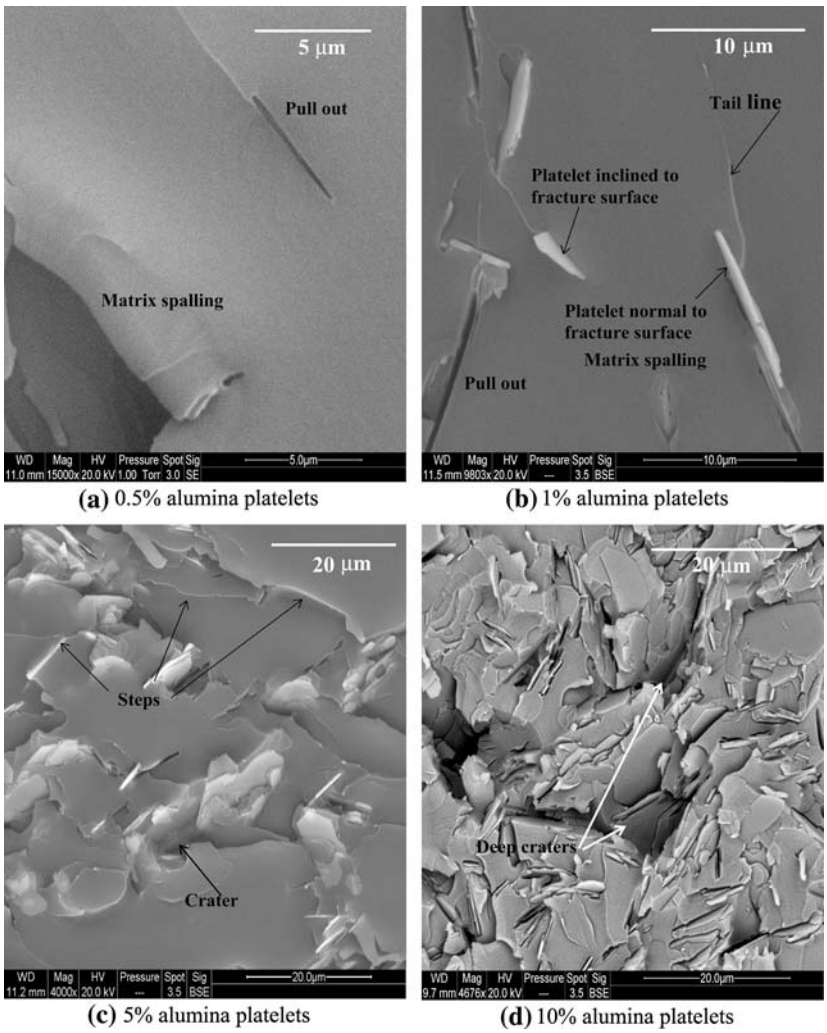

Fig. 9 SEM micrographs showing detailed features on the fracture surface

(a) 0.5% alumina platelets **(b)** 1% alumina platelets

(c) 5% alumina platelets **(d)** 10% alumina platelets

severe crack meandering and twisting (see Fig. 9c, d). When we increase the volume fraction beyond 5%, stacking of platelets occurs as shown in Fig. 2e, d. The stacked platelets may not wet-out properly and as a result there is no further improvement in toughness beyond 5% volume fraction of platelets.

Modeling

There exist theoretical models for predicting the elastic properties of composites with unidirectionally aligned reinforcements. The Halpin-Tsai [17, 18] model and the Eshelby-Mori-Tanaka [19, 20] method are the two most widely used models. The applicability of these models to the platelet-reinforced composites is explored in this section. In the composites prepared in this study, the alumina platelets are randomly oriented and are stacked together at high volume fractions (see Fig. 2). Methods mentioned above give higher estimates of moduli unless they are modified for accounting the orientation and stacking effects.

The Halpin-Tsai equation for elastic modulus of composites reinforced with unidirectionally aligned short fiber is [17]

$$E = \frac{E_m(1 + \xi\eta V_f)}{1 - \eta V_f} \tag{1}$$

where E and E_m are the elastic modulus of composite and matrix, V_f is volume fraction of alumina platelet, ξ is shape parameter depending upon filler geometry and loading direction (see Fig. 10), and η is given by

$$\eta = \frac{(E_f/E_m) - 1}{(E_f/E_m) + \xi} \tag{2}$$

where E_f is the elastic modulus of reinforcement. For modeling the elastic behavior of nanocomposites, the polygonal shaped platelets have been idealized to be of disc

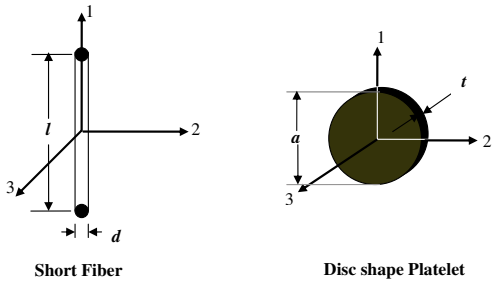

Loading direction	Composite modulus		Shape parameter	
	Fiber	Platelet	Fiber	Platelet
1	$E_{11} = E_l$	$E_{11} = E_l$	$\xi = 2(l/d)$	$\xi = 2(a/t)$
2	$E_{22} = E_t$	$E_{22} = E_l$	$\xi = 2$	$\xi = 2(a/t)$
3	$E_{33} = E_t$	$E_{33} = E_t$	$\xi = 2$	$\xi = 2$

Fig. 10 Coordinate system and shape parameter for short fibers and disk shape platelets. (E_l and E_t denote the longitudinal and transverse elastic moduli, l and d are the length and diameter of fiber, a and t are the diameter and thickness of disc)

shape with average diameter of 7.5 μm and thickness of 200 nm. Elastic modulus and Poisson's ratio of reinforcement alumina platelets and epoxy matrix were taken to be (375 GPa, 0.23) and (3.82 GPa, 0.35) respectively. Coordinate system and shape parameters for different loading directions are shown Fig. 10.

Complete alignment of platelets can take place in two ways—(1) all the platelet planes are normal to the direction of applied load or (2) all the platelet planes are parallel to the direction of applied load. In both these cases equation (1) can be used to estimate the elastic modulus of the nanocomposite. Modulus thus obtained is denoted by $E_\perp$ and $E_{||}$ respectively. Modulus of composite with randomly oriented platelets is obtained by Eq. 3 proposed by by van Es et al. [21].

$$E_{\text{ran}-3D}^{\text{platelets}} = 0.49E_{||} + 0.51E_\perp \tag{3}$$

The composite elastic modulus thus obtained is shown in Fig. 11 along with the experimental values. This approach is able to capture the effect of platelets on elastic modulus at low volume fractions, but considerably overestimate the effect at high volume fraction of alumina platelets as can be seen in Fig. 11 (line labeled HT). The difference between the predicted value and experimental value of elastic modulus at higher volume fractions is due to the effect of stacking of platelets, which is not accounted in the model. Stacking reduces the aspect ratio of the reinforcements and reduces $E_{||}$.

From the SEM micrographs, it was observed that, on an average, two platelets stacked together at 5% of volume fraction and 3–4 platelets stacked together in case of 10% volume fraction. Based on this the aspect ratio was corrected in calculating $E_{||}$ for these volume fractions. The value of elastic modulus thus obtained has much lower deviation from the experimental value as can be seen from Fig. 11 (see line labeled HT-stacking).

Eshelby determined the effect of ellipsoidal inclusion in an infinite matrix on the elastic field [19]. Mori-Tanaka later derived the average stress using the principles of Eshelby's inclusion model for a non-dilute mixture of spheroidal inclusion in a matrix. Later Tandon and Weng [22] calculated the effective moduli of a unidirectionally aligned two-phase composite reinforced by spheroidal inclusions using Mori-Tanaka method. Elastic moduli obtained by them can be written as

$$E_{11} = E_{||} = \frac{2AE_m}{2A + V_f[-2\nu A_3 + (1-\nu)A_4 + (1+\nu)A_5 A]} \tag{5}$$

and

$$E_{33} = E_\perp = \frac{AE_m}{A + V_f(A_1 + 2\nu A_2)} \tag{6}$$

where ν is the Poisson's ratio of the matrix and A, A_1, A_2, A_3, A_4 and A_5 are the function of the properties of the filler and the matrix and Eshelby's tensor. Complete details of these equations can be found elsewhere [22, 23].

Elastic modulus, calculated using Eqs. 3, 5 and 6 with and without stacking effects is shown in Fig. 11. It can be easily seen that the predicted value of elastic modulus by Mori-Tanaka method is closer to experimental values than that predicted by Halpin-Tsai model even for high volume fraction of platelets. A comparison of elastic moduli obtained by these two methods is also given in Table 1.

The Haplin-Tsai model is an empirical model and does not account for the effects of interaction between the reinforcements, which is significant at higher volume fractions. The Mori-Tanaka method is superior in this respect, but still over estimate the elastic modulus by 15% for the 10% platelet composite. We believe that at higher volume fractions, in addition to the stacking effects, the resin may not wet the platelets properly and therefore their effectiveness in constraining the matrix deformation decreases resulting in lower elastic modulus.

Conclusions

Epoxy composites were prepared by dispersing 200 nm thick alumina platelets as reinforcements in epoxy through ultrasonication technique. The results of material characterization indicate the following.

- SEM images of the nanocomposites show good dispersion of the alumina platelets in the matrix.

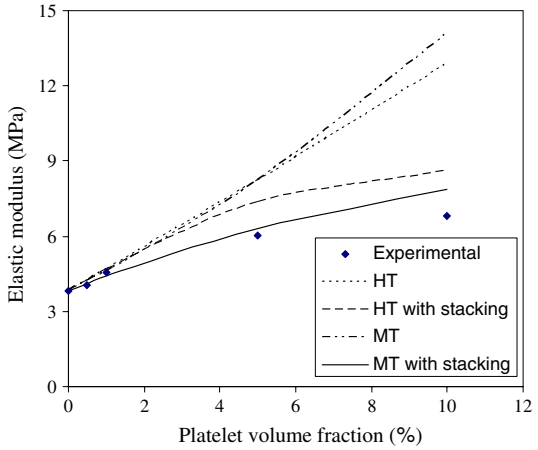

Fig. 11 Experimental and predicted results based on Halpin-Tsai and Mori-Tanaka model for composite elastic modulus

Table 1 Comparison of elastic modulus

Volume fraction (%)	Elastic modulus (GPa)				
	Experimental	Halpin-Tsai	Difference (%)	Mori-Tanaka	Difference (%)
0	3.82	3.82	–	3.82	–
0.5	4.04	4.25	5.2	4.11	1.7
1	4.55	4.68	2.9	4.39	–3.5
5	6.03	7.35	21.9	6.32	4.8
10	6.79	8.61	26.8	7.85	15.6

Stacking is observed only at higher volume fraction (above 5%) of platelets.

- For 10% loading of alumina platelets, there is a significant improvement of 110% in fracture toughness and 78% in elastic modulus of the nanocomposites where as tensile strength and failure strain decreased by 53% and 73%.
- SEM micrographs of the fracture surfaces indicates the presence of mechanisms such as platelet pull out, tail marks, crater formation and spalling of the matrix at the platelet sites.
- The estimates of elastic modulus using Mori-Tanaka method with modifications for orientation and stacking of platelets matches well with the experimental result.

Even though at 10% platelet volume fraction, the tensile strength and failure strain of epoxy reduces considerably, the 1% composite still has good tensile strength and fracture toughness with moderate increase in elastic modulus. At this volume fraction of the platelet it can be concluded that the composite has improved overall properties compared to epoxy.

Acknowledgements The authors acknowledge the financial support of Aeronautical Research and Development Board, India (ARDB/AE/19990054) and Ministry of Human Resource Development, India (MHRD-ME-TAT-20030334). We also acknowledge Department of Science and Technology, India (DST/INT/US-NSF/RPO-159/04) for the financial support under the INDO-US collaboration program.

References

1. Kojima Y, Usuki A, Kawasumi M, Okada A, Kurauchi T, Kamigaito O (1993) J Appl Polym Sci 49:1259
2. Kojima Y, Usuki A, Kawasumi M, Okada A, Kurauchi T, Kamigaito O (1993) J Mater Res 8:1185
3. Agag T, Koga T, Takeichi T (2001) Polymer 42:3399
4. Chen TK, Tien YI, Wei KH (2000) Polymer 41:1345
5. Daniel IM, Miyagawa H, Gdoutos EE, Luo JJ (2003) Exp Mech 43:348
6. Sue HJ, Gam KT, Bestaoui N, Clearfield A, Miyamoto M, Miyatake N (2004) Acta Mater 52:2239
7. Xiaodong L, Hongsheng G, Scrivens AW, Dongling F, Thakur V, Sutton MA, Reynolds AP, Myrick ML (2005) Nanotechnology 16:2020
8. Chisholm N, Mahfuz H, Rangari VK, Ashfaq A, Jeelani S (2005) Comp Struct 67:115
9. Park SS, Bernet N, Roche DL, Hahn HT (2003) J Comp Mat 37:465
10. Singh RP, Zhang M, Chan D (2002) J Mater Sci 37:781
11. Zhang M, Singh RP (2002) Mater Lett 58:408
12. Evora VMF, Shukla A (2003) Mater Sci Eng A 361:358
13. D638-03, Standard test method for tensile properties of plastics, Annual Book of ASTM Standards. American Society of Testing and Materials, West Conshohocken (2004)
14. D5045-99, Standard test methods for plane-strain fracture toughness and energy release rate of plastic materials, Annual Book of ASTM Standards. American Society of Testing and Materials, West Conshohocken (2004)
15. Cai H, Faber KT (1992) J Am Ceram Soc 75:3111
16. Leung CKY, Li VC (1992) J Mech Phys Solids 40(6):1333
17. Halpin JC (1969) J Comp Mat 3:732
18. Halpin JC, Kardos JL (1976) Polym Eng Sci 16:344
19. Eshelby JD (1957) Proc Roy Soc A241:376
20. Mori T, Tanaka K (1973) Acta Metall 21:571
21. van Es M, Xiqiao F, van Turnhout J, van der Giessen E (2001) Specialty polymer additives: principles and applications. Blackwell Science; Chapter 21
22. Tandon GP, Weng GJ (1984) Polym Compos 5:327
23. Hui CY, Shia D (1998) Polym Eng Sci 38:774